

Plasma enhanced chemical vapor deposition of SiO₂ using novel alkoxysilane precursors

K. H. A. Bogart, N. F. Dalleska, G. R. Bogart, and Ellen R. Fisher

Citation: *Journal of Vacuum Science & Technology A* **13**, 476 (1995); doi: 10.1116/1.579382

View online: <http://dx.doi.org/10.1116/1.579382>

View Table of Contents: <http://scitation.aip.org/content/avs/journal/jvsta/13/2?ver=pdfcov>

Published by the AVS: Science & Technology of Materials, Interfaces, and Processing

Articles you may be interested in

[Investigation of SiO₂ plasma enhanced chemical vapor deposition through tetraethoxysilane using attenuated total reflection Fourier transform infrared spectroscopy](#)

J. Vac. Sci. Technol. A **13**, 2355 (1995); 10.1116/1.579521

[Monte Carlo simulation of surface kinetics during plasma enhanced chemical vapor deposition of SiO₂ using oxygen/tetraethoxysilane chemistry](#)

J. Vac. Sci. Technol. A **11**, 2562 (1993); 10.1116/1.578607

[Determination of the mechanical stress in plasma enhanced chemical vapor deposited SiO₂ and SiN layers](#)

J. Vac. Sci. Technol. B **11**, 614 (1993); 10.1116/1.586809

[Planarization of SiO₂ films using reactive ion beam in plasma enhanced chemical vapor deposition](#)

J. Appl. Phys. **69**, 6637 (1991); 10.1063/1.348878

[Atomic structure in SiO₂ thin films deposited by remote plasma-enhanced chemical vapor deposition](#)

J. Vac. Sci. Technol. A **7**, 1136 (1989); 10.1116/1.576242

ADVERTISEMENT

Instruments for advanced science

Gas Analysis



- dynamic measurement of reaction gas streams
- catalysis and thermal analysis
- molecular beam studies
- dissolved species probes
- fermentation, environmental and ecological studies

Surface Science



- UHV TPD
- SIMS
- end point detection in ion beam etch
- elemental imaging - surface mapping

Plasma Diagnostics



- plasma source characterization
- etch and deposition process reaction kinetic studies
- analysis of neutral and radical species

Vacuum Analysis



- partial pressure measurement and control of process gases
- reactive sputter process control
- vacuum diagnostics
- vacuum coating process monitoring

contact Hiden Analytical for further details



info@hideninc.com
www.HidenAnalytical.com
CLICK to view our product catalogue 

Plasma enhanced chemical vapor deposition of SiO₂ using novel alkoxysilane precursors

K. H. A. Bogart and N. F. Dalleska

Department of Chemistry, Colorado State University, Fort Collins, Colorado 80523

G. R. Bogart

BioStar Inc., Boulder, Colorado 80301

Ellen R. Fisher

Department of Chemistry, Colorado State University, Fort Collins, Colorado 80523

(Received 10 November 1994; accepted 10 December 1994)

I. INTRODUCTION

Plasma enhanced chemical vapor deposition (PECVD) is widely used in the microelectronics industry to deposit thin films.¹ Dielectric materials such as silicon dioxide (SiO₂) are often deposited by PECVD for use as gate oxides,^{2,3} intermetal dielectrics,⁴ or passivation layers for integrated circuits.^{5,6} The main advantage of PECVD over other deposition methods such as thermal CVD⁷ is that deposition of good quality SiO₂ can be performed at low substrate temperatures (<350 °C) from SiH₄/O₂ or SiH₄/N₂O plasmas.^{8–10} These gas mixtures, however, are not desirable due to the pyrophoric nature of silane and problems with nitrogen contamination from N₂O.^{3,11}

Organosilanes, such as tetraethoxysilane (TEOS), have been used since the 1960s to deposit SiO₂ by PECVD.^{12–14} In addition to containing silicon and oxygen in a single molecule, TEOS has reduced toxicity and hazard compared to more conventional sources.^{5,7} Furthermore, TEOS provides better conformality and void free films with superior step coverage even at geometries less than 0.5 μm.^{5,15,16} These films also retain good mechanical and electrical properties at these dimensions.¹⁵ Although SiO₂ films deposited from pure TEOS show hydrocarbon incorporation in this film, addition of an oxidant such as O₂ or O₃ eliminates this film contaminant.^{11,17}

Here, we report the use of an inductively coupled rf plasma reactor to deposit SiO₂ films from pure TEOS. We have also been successful in depositing SiO₂ from the alkoxysilane precursors triethoxysilane (TriEOS), tetramethoxysilane (TMOS), and trimethoxysilane (TriMOS). These studies were undertaken for a number of reasons. First, to our knowledge, these precursors have not previously been used for PECVD of SiO₂. Thus, we wished to ascertain whether SiO₂ could be deposited from these starting materials. Second, we wanted to explore the effects of various deposition parameters on deposition rates, film refractive index, and film composition. Third, we were interested in determining whether changing the number and type of functional groups in the precursor would affect the film's properties. For example, Does decreasing the number of alkoxy substituents

decrease the amount of hydrocarbon incorporation in the films? Hydrocarbon incorporation in the SiO₂ film is not desirable because it will alter the mechanical and electrical properties of the film. Does the presence of an Si–H moiety in the precursor produce films containing residual Si–H bonds? The optical and electronic properties of the deposited materials could be strongly affected by the hydrogen content in the films.¹⁸ Finally, we are interested in the mechanism of SiO₂ film deposition. By changing the starting materials systematically, we hoped to shed light on the process by which SiO₂ is formed from alkoxysilanes.

This communication describes our results using these novel alkoxysilane precursors for PECVD of SiO₂ films in an inductively coupled rf plasma reactor. The effects of deposition time, rf power, and organosilane pressure on the films' characteristics are described.

II. EXPERIMENT

An inductively coupled rf plasma reactor, Fig. 1, was built from two glass tubes with 50 mm O-ring joints, allowing easy access to the interior of the plasma chamber. The chamber is pumped by an Edwards two-stage rotary vane pump (140 ℓ/s). An eight turn, nickel plated copper coil is used to couple 13.56 MHz rf power to the chamber and is tuned with a Jennings 100 pF variable capacitor, Fig. 1. The alkoxysilanes (25.5±0.5 °C) was admitted into the plasma chamber through a heated (39–56 °C) line. The vapor pressure was controlled using a Nupro bellows-sealed metering valve. The pressure in the chamber was monitored with an MKS Baratron capacitance manometer which is insensitive to differing gas compositions.

p-type silicon wafers (1-0-0 crystallization orientation) with 40–60 Å native oxide were used as substrates. Freshly cleaned and polished sodium chloride (NaCl) window substrates were also used. The substrates were placed on glass slides and oriented parallel to gas flow in the plasma chamber. Both a silicon wafer and a NaCl window were used for each deposition. Deposition times ranged from 0.5 to 10.0 min and were defined by when the rf power was applied. Power dependence measurements were made by varying the

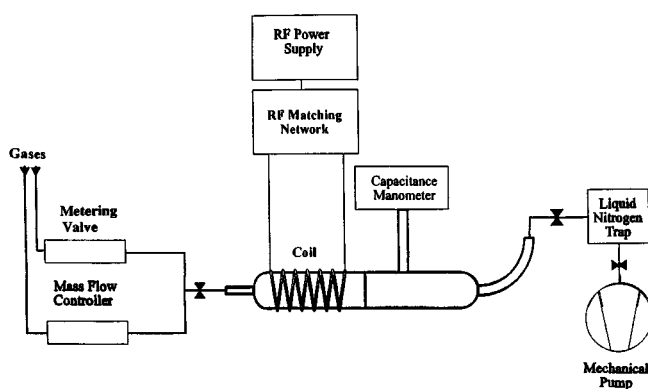


FIG. 1. Schematic diagram of the inductively coupled plasma reactor apparatus used for plasma deposition of SiO₂.

rf power from 20 to 90 W. For each measurement, deposition time was kept at 5 min for TMOS, TriMOS, and TriEOS. Three min depositions were used for TEOS due to its faster deposition rate. Pressure was varied from 20 to 32 mTorr by throttling the valve between the plasma chamber and the liquid nitrogen trap, Fig. 1. For each alkoxysilane introduced into the plasma chamber, the pressure was allowed to stabilize prior to application of the rf power. All of the alkoxysilanes (>95% pure) were purchased from United Chemical Technology and were used without further purification except for multiple freeze-pump-thaw cycles.

Substrates were removed from the plasma chamber for analysis. Transmission spectra for the NaCl substrates were obtained with a Nicolet 5PC Fourier transform infrared

(FTIR) spectrometer. Spectra shown were not manipulated unless specifically noted. Absolute absorbance values were obtained by converting transmission spectra to absorbance and performing a baseline correction on the spectra with a second order polynomial. Film thicknesses and refractive indices were calculated from ellipsometric analyses at 632.8 nm using a Gaertner L116A automatic null ellipsometer.

III. RESULTS AND DISCUSSION

Figure 2(A) shows a typical FTIR spectrum of a SiO₂ film deposited in our reactor with 100% TEOS. The absorbance bands at 2977, 2930, and 2898 cm⁻¹ are assigned to C-H stretches from aliphatic-CH₃, -CH₂, and -CH groups, respectively.^{19,20} The weak absorbances at 1445 and 1391 cm⁻¹ are the asymmetric and symmetric C-H bending of -CH₃ groups.^{19,20} The most intense absorbance band at 1078 cm⁻¹ is due to Si-O-C and linear Si-O-Si groups.^{19,20} Absorbance peaks at 967, 884, and 795 cm⁻¹ are more difficult to identify. Assignments in the literature include Si-OH and Si-O-CH₂CH₃ for the 967 cm⁻¹ band, Si-H and Si-C for the 884 cm⁻¹ band, and Si-O-Si and Si-O-(CH₃)_{x=1,2} for the 795 cm⁻¹ band.^{17,19-21} The doublet at 2342 and 2359 cm⁻¹ is due to residual carbon dioxide not purged from the FTIR spectrometer. The spectra for SiO₂ films deposited from TEOS in our reactor are very similar to those found in the literature.^{17,21}

Figure 2(B) shows a FTIR spectrum for the SiO₂ film deposited with a 100% TriEOS plasma. The spectral features are very similar to those of the film deposited from TEOS with respect to the aliphatic hydrocarbon and silicon oxide absorbance peaks, Fig. 2(A). The most noticeable difference

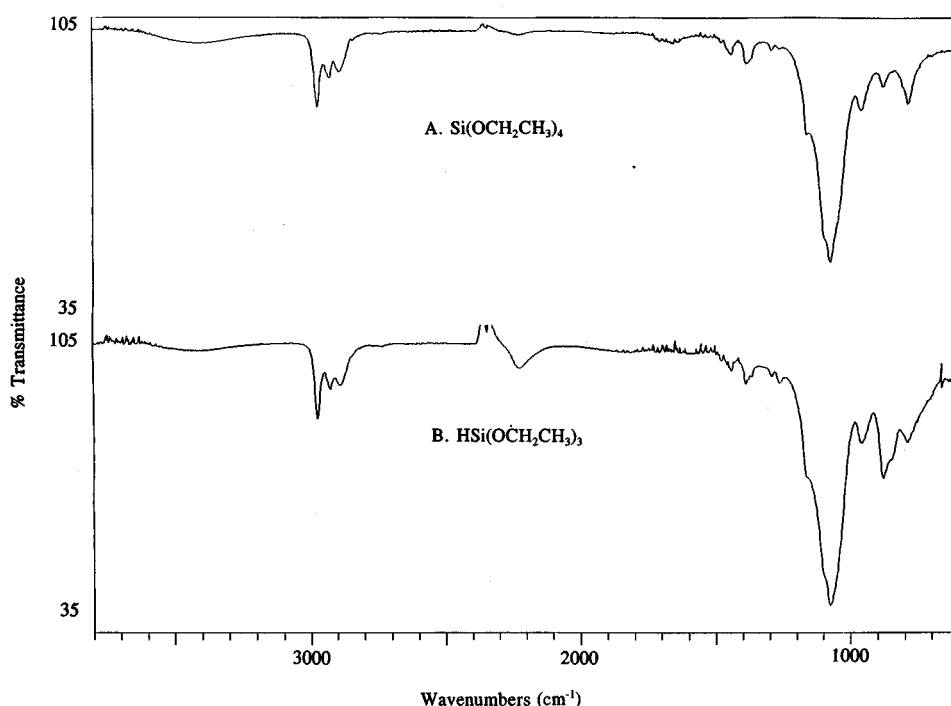


FIG. 2. FTIR transmission spectra of films deposited on NaCl windows using (A) 100% TEOS and (B) 100% TriEOS. A baseline correction with a second-order polynomial was performed on the TriEOS spectrum. Deposition conditions for these spectra are given in Table I.

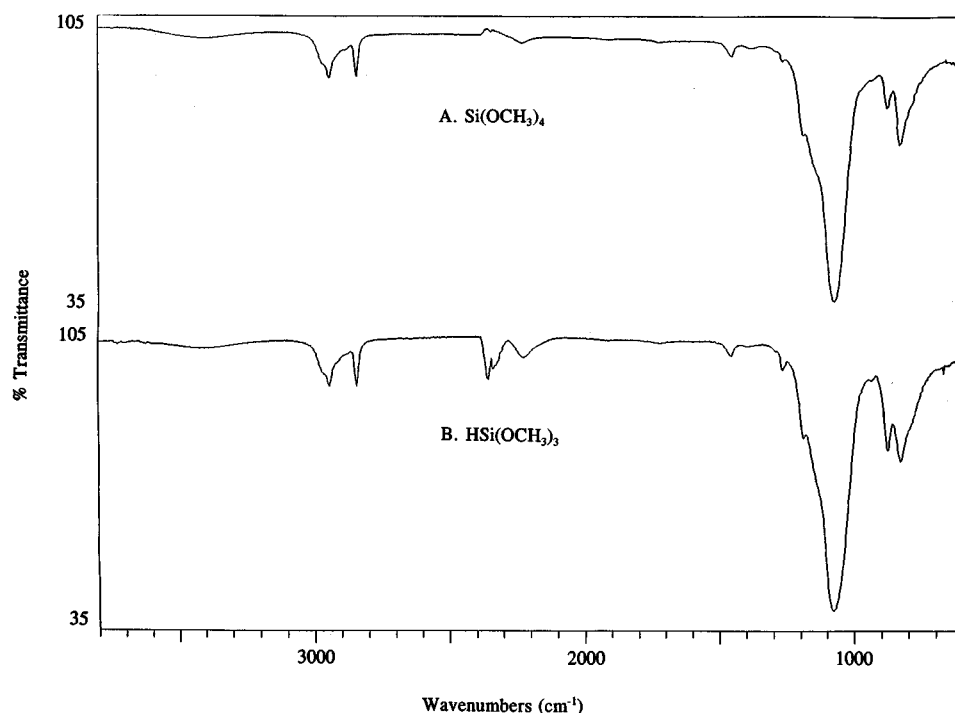


FIG. 3. FTIR transmission spectra of films deposited on NaCl windows using (A) 100% TMOS and (B) 100% TriMOS. Deposition conditions for these spectra are given in Table I.

is the presence of the Si–H stretching absorbance at 2230 cm^{-1} .^{19–21} This absorbance band is not seen with TEOS, Fig. 2(A). The other significant difference is the increased intensity for the absorbance peak at 880 cm^{-1} and the presence of a shoulder at a lower frequency.

The FTIR spectrum for a film deposited from a 100% TMOS plasma is shown in Fig. 3(A). Again, the spectral features are similar to those for TEOS films, indicating we have deposited SiO₂. There are, however, a few notable differences in the two spectra. The most marked change is the absence of the aliphatic C–H stretching vibration for the –CH₂ group. Other changes include the presence of a very weak Si–H absorbance peak at 2230 cm^{-1} , the absence of the Si–O absorbance peak near 980 cm^{-1} , and an additional absorbance peak at 835 cm^{-1} .

Figure 3(B) shows the FTIR spectrum of the film deposited from a 100% TriMOS plasma. The spectral features are nearly identical to those for the film deposited from TMOS, again indicating that we are indeed depositing SiO₂. The Si–H stretching vibration is observed in this film, similar to films using TriEOS as a precursor, Fig. 2(B). The absorbance peak intensity at 2230 cm^{-1} is much greater for TriMOS than for TMOS, but is almost equal in intensity to that for the TriEOS film.

Table I lists deposition rates and refractive indices for SiO₂ films deposited from TEOS, TriEOS, TMOS, and TriMOS in our reactor at the deposition conditions noted in Table I. Deposition rates for the ethoxysilanes are greater than 978 Å/min , while those for the methoxysilanes are much lower at $<790\text{ Å/min}$. We have not found any pub-

TABLE I. Deposition rates, refractive indices, and FTIR absorbance values for SiO₂ films.^a

Alkoxysilane		Deposition rate (Å/min)	Refractive index	FTIR absorbance values ^b					
				CH ₃	CH ₂	CH	SiO	SiH	SiO/CH ₃
TEOS	Avg	1360	1.463	6.6	3.4	3.1	27.1	0.0	4.14
	<i>s_d</i>	111.3	0.0047	0.7	0.6	0.6	0.7	0.0	0.477
TriEOS	Avg	1060	1.459	7.8	4.5	4.0	35.4	1.8	4.59
	<i>s_d</i>	73.3	0.0017	0.9	0.6	0.5	1.8	0.2	0.331
TMOS	Avg	610.7	1.450	4.2	0.0	4.0	36.2	0.2	8.56
	<i>s_d</i>	109.5	0.0155	0.6	0.0	0.7	4.8	0.2	0.168
TriMOS	Avg	745.7	1.446	4.5	0.0	4.5	37.9	1.2	8.42
	<i>s_{s,d}</i>	38.8	0.002	0.2	0.0	0.2	1.6	0.3	0.031

^aThese films were all deposited under the following deposition conditions: rf input power=50 W; reactor pressure=28–48 mTorr; deposition time=3 min for TEOS, 5 min for other alkoxysilanes. Values given are averages of three independent depositions. Standard deviations are given, *s_d*.

^bAbsorbance $\times 10^{-2}$.

lished deposition rates for 100% TEOS depositions; however, our deposition rates are equal to or greater than deposition rates published for TEOS/O₂ plasma depositions.^{3,12,20}

The refractive indices for TEOS and TriEOS films, Table I, are identical to published values for chemically deposited SiO₂, 1.44 to 1.46.¹ Our values also agree with literature values for the refractive index of SiO₂ films deposited by PECVD from TEOS, which vary from 1.45 to 1.55.¹ The SiO₂ films grown from TMOS and TriMOS have refractive indices in the same range, 1.450 and 1.446, respectively. Variations in refractive index may be due to film species other than SiO₂. For example, the refractive index of non-crystalline Si-O is approximately 1.95 at 633 nm (Ref. 22) and is 1.4 to 1.5 for hydrocarbons.²³ Our measured refractive indices could be a combination of values for various species in the deposited film.

Also listed in Table I are the FTIR absorbance values for the -CH₃, -CH₂, Si-O, and Si-H stretching absorption bands and the ratio of the Si-O to -CH₃ absorbance values for the depositions performed with all four alkoxy silanes. The absolute absorbance values for the Si-O peaks are greater for the methoxy silanes than for the ethoxy silanes by approximately 15%. The values of the -CH₃ absorbance peak are nearly 40% less for the methoxy silanes compared to the ethoxy silanes. Furthermore, the methylene absorbance at 2930 cm⁻¹ is present in the ethoxy silane films but is absent in the methoxy silane films. As noted above, the films deposited from trialkoxy silanes show a marked increase in the values of the Si-H absorbance at 2230 cm⁻¹ (~0.015 abs) as compared to that for films deposited from the tetraalkoxy silanes (~0.002 abs). The ratio of the Si-O to -CH₃ absorbance values is approximately 4.4 for the ethoxy silanes and is 8.5 for the methoxy silanes. From these data, we conclude that the SiO₂ films grown from the methoxy silanes have a smaller degree of hydrocarbon incorporation than those grown from the ethoxy silanes. The lesser amount of carbon and hydrogen in the methyl substituent may simply give less hydrocarbon incorporation in the SiO₂ films.

Deposition time, rf power, and alkoxy silane pressure were varied to determine each of their effects on deposition rate, refractive index, and FTIR absorbance values for the -CH₃, -CH₂, and Si-O peaks. Although we do not explicitly show all these data here, we will discuss the trends observed in varying these plasma parameters.²⁴ We found that as deposition time increases, deposition rates decrease slightly and appear to level off for all four alkoxy silanes. This pattern may indicate that a steady state deposition is not immediate in the plasma reactor but is achieved within a few minutes. Published data for TEOS/O₂ plasmas show the deposition rate to be independent of deposition time over a time range of several minutes to hours.^{13,14,20} Our high deposition rate, ~1360 Å/min for TEOS, allows us to study deposition rates at times less than 10 min. As deposition time is increased, the refractive indices for the four alkoxy silanes remain constant. Absorbance values for the alkane and silicon oxide bands increase as deposition time increases, indicating a thicker film. There is not a significant change in the ratio of Si-O to -CH₃ absorbance values with increased deposition time.

As the rf power is increased, deposition rates of the four

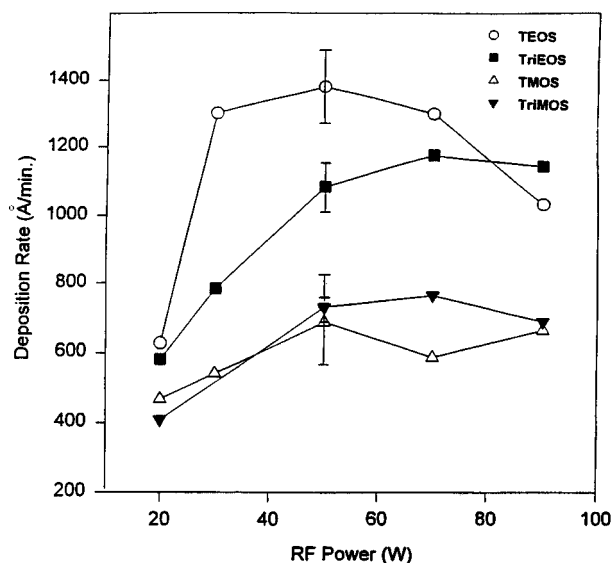


Fig. 4. Relation between rf input power and deposition rate for the four alkoxy silanes used to deposit SiO₂ films. Open circles are data for the TEOS depositions, closed squares are for the TriEOS depositions, open triangles are for TMOS depositions, and closed, inverted triangles are for TriMOS depositions. Vertical lines represent the standard deviation in the experimental values. Deposition conditions for all four alkoxy silanes were essentially the same, Table I.

alkoxy silanes increase and tend to level off or decrease, Fig. 4. Maxima for the curves indicate an optimal power to maximize deposition rate. For TEOS plasmas, the optimal rf power is between 30 and 70 W. The other alkoxy silane plasmas maximize deposition rate between 50 and 90 W of rf power. Too low an rf power may not create as many reactive species for deposition. At higher rf powers, the deposition rate does not continue to increase. At these higher powers, the reaction may be limited by other factors in the system such as decomposition of the reactive species in the plasma chamber. The index of refraction of the deposited SiO₂ films remains constant as rf power is varied from 20 to 90 W. The FTIR absorbance values for the alkane and silicon oxide stretching absorption bands increase and then decrease as power increases. As rf power increases, absorbance values, hence film thickness, follows the same pattern as deposition rate, Fig. 4.

Changing the alkoxy silane pressure from 20 to 324 mTorr in the plasma chamber has little effect on the film characteristics investigated, including deposition rate and refractive index, for all four alkoxy silanes. Our results suggest that the alkoxy silane vapor pressure in our reactor is not a limiting factor for the deposition process. The FTIR absorbance values for the films also did not change significantly as pressure was varied.

These results show that SiO₂ can indeed be deposited from these new alkoxy silane precursors. Subtle differences in the deposited films are, however, evident between the four alkoxy silanes studied and these differences give us insight into the deposition mechanism. For example, the FTIR spectra show the presence of a methylene absorbance in the films deposited from the ethoxy silanes. This absorbance is *not* present in the films deposited from the methoxy silanes. This

indicates that the deposition process is not disrupting the methyl group to form a -CH₂ moiety in the film. Furthermore, this could imply that the ethyl group from the ethoxysilanes is also left intact during deposition. Several studies in the literature hypothesize that the C-O bonds in the alkoxy silanes are ruptured in the plasma forming Si-O and C_xH_{2x-1} species.^{7,17} The C-O bond (100.9 kcal/mol) is weaker than the Si-O bond (130.9 kcal/mol).²⁵ Thus, this is a plausible decomposition pathway on the basis of thermochemical arguments. Thermal decomposition studies of TEOS also indicate that gas-phase decomposition products include organic fragments such as ethanol, ethylene, and methane.^{7,17,26} Our data support the hypothesis that the alkyl moieties are separated from the silicon oxygen group as the intact alkane radical.

Another important feature in our FTIR spectra is the Si-H absorbance at 2230 cm⁻¹. Fracassi *et al.* have reported the absence of the Si-H absorbance band in their films deposited from 100% TEOS.¹⁷ In contrast, several other groups report the presence of a Si-H absorbance band in the FTIR spectra of their TEOS and TEOS/O₂ plasma films.^{14,20,21} Our results do not show a distinct Si-H absorbance for the tetraalkoxy silane films. The strong intensity of the Si-H absorbance band does, however, indicate the presence of Si-H species in the films formed from the trialkoxy silane precursors, Figs. 2(B) and 3(B). This implies that, although the Si-H bond is relatively weak (~99 kcal/mol) (Ref. 25) when compared to the Si-O bond (~131 kcal/mol),²⁵ it is not completely dissociated in the plasma deposition process. It also suggests that Si-H bonding in the films is *not* formed from the hydrogen atoms in the alkane substituents. This also supports the proposed deposition mechanism^{7,17,26} of preferentially breaking the C-O bond in the alkoxy silane and producing C₂H₅ or CH₃ radicals to breaking the Si-O or Si-H bonds.

IV. CONCLUSIONS

In summary, we have deposited SiO₂ films on silicon and NaCl substrates from TEOS and three novel alkoxy silanes, TriEOS, TMOS, and TriMOS. The films from all four alkoxy silanes have FTIR spectra and refractive indices similar to SiO₂, and deposition rates are reasonably fast, ~1360 Å/min for TEOS. As the size of the alkane substituent decreases, the amount of hydrocarbon incorporation in the films decreases. Films deposited with trialkoxy silanes show significant amounts of Si-H bonding in their FTIR spectra, while those

deposited from tetraalkoxy silanes do not. The methoxy silanes give films with a greater SiO/CH₃ ratio but at a slower deposition rate. Future investigations will continue to explore PECVD of SiO₂ from novel alkoxy silane precursors, including ClSi(OC₂H₅)₃.

ACKNOWLEDGMENTS

The support of the National Science Foundation under Grant No. DMR-9409272, Sandia National Laboratories under Contract No. AJ-3848 and Colorado State University through the Faculty Diversity Career Enhancement Fund and Faculty Research Grants is gratefully acknowledged.

¹A. C. Adams, in *Plasma Deposited Thin Films*, edited by J. Mort and F. Jansen (Chemical Rubber, Boca Raton, 1986).

²G. W. Hills, A. S. Harris, and M. J. Thoma, *Solid State Technol.* April, 127 (1990).

³I. T. Emesh, G. D'Asti, J. S. Mercier, and P. Leung, *J. Electrochem. Soc.* **136**, 3404 (1989).

⁴L. Chen, S. Hsia, and K. Chen, *Jpn. J. Appl. Phys.* **32**, 6119 (1993).

⁵G. Tochitani, M. Shimosuma, and H. Tagashira, *J. Vac. Sci. Technol. B* **11**, 400 (1993).

⁶A. Banerjee and T. DebRoy, *J. Vac. Sci. Technol. B* **10**, 3395 (1992).

⁷J. E. Crowell, L. L. Tedder, H.-C. Cho, F. M. Cascarano, and M. A. Logan, *J. Electron. Spectrosc. Rel. Phenom.* **54/55**, 1097 (1990).

⁸A. C. Adams, F. B. Alexander, C. D. Capio, and T. E. Smith, *J. Electrochem. Soc.* **28**, 1545 (1981); S. V. Hattangady, R. G. Alley, G. G. Fountain, R. J. Markunas, G. Lucovsky, and D. Temple, *J. Appl. Phys.* **73**, 7635 (1993).

⁹D. L. Smith and A. S. Alimonda, *J. Electrochem. Soc.* **140**, 1496 (1993).

¹⁰S. W. Hsieh, C. Y. Chang, and S. C. Hus, *J. Appl. Phys.* **74**, 2636 (1993).

¹¹M. G. J. Veprek-Heijman, and D. Boutard, *J. Electrochem. Soc.* **138**, 2042 (1991).

¹²E. B. Priestley and P. J. Call, *Thin Solid Films* **69**, 39 (1980).

¹³D. R. Secrist and J. D. Mackenzie, *J. Electrochem. Soc.* **113**, 914 (1966).

¹⁴S. W. Ing, Jr. and W. Davern, *J. Electrochem. Soc.* **112**, 284 (1965).

¹⁵K. Maeda and S. M. Fisher, *Solid State Technol.* June, 83 (1993).

¹⁶A. S. Harrus, G. W. Hills, and M. J. Thoma, *Pure Appl. Chem.* **9**, 1757 (1990).

¹⁷F. Fracassi, R. d'Agostino, and P. Favia, *J. Electrochem. Soc.* **139**, 2636 (1992).

¹⁸N. M. Johnson, C. E. Nebel, P. V. Santos, W. B. Jackson, R. A. Street, K. S. Stevens, and J. Walker, *Appl. Phys. Lett.* **59**, 1443 (1991).

¹⁹R. T. Conley, *Infrared Spectroscopy* (Allyn & Bacon, Boston, MA, 1966).

²⁰S. P. Mukherjee and P. E. Evans, *Thin Solid Films* **14**, 105 (1972).

²¹U. Mackens and U. Merkt, *Thin Solid Films* **97**, 53 (1982).

²²*Handbook of Optical Constants of Solids*, edited by E. D. Palik (Academic, Orlando, 1985).

²³*Handbook of Chemistry and Physics*, 63rd ed., edited by R. C. Weast (Chemical Rubber, Boca Raton, 1982).

²⁴A more detailed presentation of this data will be given in a future publication. K. H. A. Bogart and E. R. Fisher (unpublished).

²⁵P. Ho and C. F. Melius (unpublished).

²⁶M. G. M. Van der Vis, E. H. P. Cordfunke, and R. J. M. Konings, *J. Phys. (Paris) IV* **3**, 75 (1993).